ORIGINAL PAPER

Energy and time optimization during exit from torpor in vertebrate endotherms

Pedro Goes Nogueira-de-Sá[1] · José Eduardo Pereira Wilken Bicudo[2] · José Guilherme Chaui-Berlinck[1]

Abstract

Torpor is used in small sized birds and mammals as an energy conservation trait. Considerable effort has been put towards elucidating the mechanisms underlying its entry and maintenance, but little attention has been paid regarding the exit. Firstly, we demonstrate that the arousal phase has a stereotyped dynamic: there is a sharp increase in metabolic rate followed by an increase in body temperature and, then, a damped oscillation in body temperature and metabolism. Moreover, the metabolic peak is around two-fold greater than the corresponding euthermic resting metabolic rate. We then hypothesized that either time or energy could be crucial variables to this event and constructed a model from a collection of first principles of physiology, control engineering and thermodynamics. From the model, we show that the stereotyped pattern of the arousal is a solution to save both time and energy. We extended the analysis to the scaling of the use of torpor by endotherms and show that variables related to the control system of body temperature emerge as relevant to the arousal dynamics. In this sense, the stereotyped dynamics of the arousal phase necessitates a certain profile of these variables which is not maintained as body size increases.

Keywords Torpor · Hibernation · Energy · Thermodynamics · Modelling · Optimization

Introduction

To keep a high body temperature under adverse environmental conditions is energetically costly to endotherms in general and particularly for the small-sized ones. For these, the alternative to undergo torpor is a beneficial option to promote survival (Wang and Wolowyk 1988; Heldmaier et al. 2004; Dausmann and Warnecke 2016; Staples 2016; Geiser et al. 2017). Torpor encompasses, albeit in a somewhat confusing nomenclature (Cheng 2008; Mohr et al. 2020), hibernation and daily torpor, and the main differences between them are a more intense metabolic downregulation and longer time-frame in the former, as well as the seasonality of the former. Therefore, birds and mammals which

undergo torpor abandon euthermia and downregulate their metabolic rate to reach lower values accompanied by a fall in body temperature (Heldmaier and Ruf 1992; Nogueira de Sá and Chaui-Berlinck 2022) whilst maintaining a steady state condition which may last for several hours, in the case of daily torpor bouts, or for days, weeks and even months, in the case of hibernators.

Descriptive features of the arousal

From a general perspective, during the entry into a torpor bout, body temperature and metabolic rate drop until they reach a new steady-state and, during arousal, they start to change again, reaching back values close to the previous euthermic condition (e.g., Heldmaier et al. 2004; Geiser 2004; Mohr et al. 2020).

Although considerable effort has been put towards elucidating the possible mechanisms underlying entry into torpor and its maintenance (Geiser 2004; Brown et al. 2007; Swoap 2008; Ruf and Geiser 2015; Staples 2016), little attention has been paid regarding the possible mechanisms which may underlie its exit. Such an exit seems to obey a somewhat

Communicated by G. Heldmaier.

✉ José Guilherme Chaui-Berlinck
jgcb@usp.br

1 Departamento de Fisiologia, Instituto de Biociências, Universidade de São Paulo, São Paulo, SP, Brasil

2 School of Earth, Atmospheric and Life Sciences, University of Wollongong, Wollongong, Australia

stereotyped dynamics, as described by several authors. For instance:

- "During an arousal, oxygen uptake showed an exponential increase to its peak, followed by a slight decline to a stable plateau … This pattern of oxygen consumption and activity corresponds with that found by Kayser (1965) who showed that the plateau in oxygen consumption corresponded with rectal temperature of 37 °C … Similarly, Wang (1978) showed that maximal heat loss (and presumably body temperature) in arousing *S. richardsonii* was not attained slightly after oxygen consumption plateaued … This phase may last from < 1 h in the bat, *Eptesicus fuscus* (Hayward and Ball, 1966) to ca. 2 h in the ground squirrel …" (Thomas et al. 1990)
- "Arousal was characterized by a metabolic rate overshoot and a rise of body temperature, followed by postarousal with rest metabolic rate and normothermic body temperature of ± 35 °C, usually lasting for only a few hours …" (Song et al. 1997)
- "The shape of this arousal curve, with an initial exponential increase in metabolism, an overshoot, and then an exponential decrease to normal resting levels, is typical of that seen during arousal from torpor in other mammal species." (Webb and Ellison 1998)
- "Interestingly, one parameter was unchanged by ambient temperature, the temperature gain index. For all ambient temperatures, squirrels reached maximal rewarming rates when they had generated 30–40% of the heat required to reach a euthermic body temperature." (Utz et al. 2007)
- "However, when the time to rewarm from a body temperature of 5–30 °C was compared, there was no difference among ambient temperature groups". (Karpovich et al. 2009)

Very similar descriptions of metabolic rate and body temperature profiles during the arousal phase can be found in many other references (e.g., Song et al. 1995; Heldmaier et al. 2004; Sprenger and Milsom 2022), and thus we go to the next step in the analysis.

Quantitative features of the arousal

To migrate from these qualitative descriptions to gain a more quantitative overview of the exit from the torpid state, we examined published graphical data and results encompassing the arousal phase. From these procedures, Table 1 and Fig. 1 were generated. The following relationships were then found.

As expected, due to the extensive nature of energy and the more pronounced drops in body temperature during hibernation (mean $T_b = 9.2$ °C), there is a significant relation between body mass and time to metabolic peak in hibernation (scaling exponent = 0.29 (0.10–0.47), p-value = 0.0008, $r^2 = 0.71$). This scaling rule results in about $t_{peak} = 25 \cdot M_b^{0.29}$ minutes in the mass range from 5 to 800 g to attain metabolic peak, which represents a time frame from 50 to 180 min. On the other hand, daily torpor did not show such a significant relationship between time to metabolic peak and body mass (scaling exponent = 0.05, p-value = 0.77, $r^2 = 0.006$), and the mean time to peak is 78.5 min. In daily torpor, mean $T_b = 18.2$ °C. These results confirm the textual descriptions of the arousal time presented before and one can assume the exit phase to take something between 1 and 2 h (Fig. 1A).

Next, we examined the association between the time to metabolic peak and the time to rewarm (i.e., the time to attain body temperature near the previous euthermic levels). Clearly, unless for some plots where the time scale did not allow for sharp distinction between the metabolic and the thermic events, the time to the metabolic peak precedes the time to complete rewarming. However, there is no correlation between these times, i.e., the time difference Δt is somewhat fixed: non-significant regression between Δt vs time to peak (slope = − 0.08, p-value = 0.59, $r^2 = 0.012$, see Fig. 1B). The mean value from the metabolic peak to the rewarming time is 23 min. Once again, this reassures the textual description of the arousal presented earlier.

Finally, we considered the value of the metabolic peak and two important points emerge from the analysis. First, there is a ratio between the metabolic peak and the euthermic resting metabolic rate. Second, this ratio does not depend either on the mass of the animal (non-significant regression with slope = 0.13, p-value = 0.54, $r^2 = 0.017$) or on the status (hibernation or daily torpor, p-value for t-test between the groups = 0.74). The ratio has a mean value of 2.09 ± 0.20. Therefore, not only these results confirm the description of a metabolic peak in the arousal phase but they also indicate that a ratio of $M_{peak} \cong 2 \cdot M_E$ composes this metabolic overshoot.

The stereotyped pattern of arousal from torpor

In short, the exit has a somewhat stereotyped dynamic characterized by a sudden increase in both metabolic rate and body temperature followed by several drops and rises until a euthermic steady-state is reached. The peak in metabolic rate is 2 times higher than the euthermic resting metabolic rate. Furthermore, the exit from torpor is a considerably faster process than the entry—while the full torpid state will be attained many hours after the onset of the metabolic downregulation, arousal takes about 1–2 h to reach a metabolic peak and, then, to go to values close to the euthermic body temperature (see, for instance, a detailed description of the arousal phase in terms of body temperature, oxygen

Table 1 Rewarming data retrieved from the literature

Species	Body mass	Status	T_{torpid}	T_E	RwT	M_E	M_{peak}	Ratio	Time to peak	References
Myotis lucifugus	6.6	H	5	37	44	41.9	74.3	1.8	38	Thomas et al. (1990)
Glossophaga soricine	10	T	22	33	200	17.9	34.1	1.9	81	Kelm and Von Helversen (2007)
Mus musculus	20	T	24	35	70	5.6	16.7	3.0	45	Swoap (2008)
Sminthopsis macroura	23.2	T	19.5	35	75	16.7	36.3	2.2	55	Geiser et al. (2014)
	24.7	T	21	33	60	14.0	33.5	2.4	50	Geiser et al. (1996)
	25	T	19	30	130	11.7	21.2	1.8	115	Geiser et al. (1998)
	25	T	17	31	80	16.7	31.3	1.9	80	Geiser (2004)
	28	T	21	32	100	12.3	22.3	1.8	100	Song et al. (1995)
Phodopus sungorus	24.5	T	14	35	130	19.0	30.7	1.6	100	Ruf and Heldmaier (1992)
	30	T	17	35	80	21.7	36.7	1.7	55	Heldmaier and Ruf (1992)
	30	H	21	35.5	90	18.4	35.2	1.9	60	Heldmaier et al. (1999)
	30.8	T	19	33	120	13.4	30.1	2.3	100	Heldmaier et al. (2004)
Phalaenoptilus nuttallii	35	T	19	37	110	11.7	24.6	2.1	95	Withers (1977)
Cercartetus nanus	36.2	H	21	35	120	10.0	20.7	2.1	60	Song et al. (1997)
	36.7	T	15	35	80	16.7	34.1	2.0	80	Westman and Geiser (2004)
		T	20	33	50	15.6	25.1	1.6	50	
Elephantulus rozeti	43	T	17	37	70	13.4	30.1	2.3	50	Lovegrove et al. (2001)
		T	10	38	150	14.0	28.5	2.0	120	
Eliomys quercinus	110	H	5	37	150	10.2	18.8	1.9	140	Ruf et al. (2021)
Glis glis	135	T	16	36	120	6.2	15.7	2.5	80	Wilz and Heldmaier (2000)
		H	5	31	180	6.2	22.7	3.7	180	
Citellus lateralis	202	H	7	36	150	15.1	26.7	1.8	120	Hammel et al. (1968)
Erinaceus europaeus	505	H	7	34	153	11.3	24.5	2.2	120	Webb and Ellison (1998)
Spermophilus parryii kennicottii	800	H	3	35	150	6.7	11.2	1.7	137	Karpovich et al. (2009)

Status: daily torpor (T) or hibernation (H). Body mass in grams; T_{torpid}: torpid body temperature and T_E: euthermic body temperature both in °C; RwT: rewarming time (minutes); euthermic resting metabolic rate (E) and peak metabolic rate in mW g^{-1}; ratio is the ratio between metabolic peak (M_{peak}) and euthermic metabolic rate (M_E): M_{peak}/M_E; time to metabolic peak in minutes

consumption, carbon dioxide production and ventilatory rates, times and timing among them in (Sprenger and Milsom 2022)).

From these preliminaries analyses, we construct idealized curves representing body temperature and metabolic rate during the exit phase from the torpid state. This is illustrated in Fig. 2.

At this point, it is important to keep in mind that the increase in metabolic rate, i.e., the metabolic peak, to a value of $2 \cdot M_E$ implies that the body temperature setpoint must present an initial period of upregulation that leads to very fast changes in the reference temperature, a topic to be dealt later on (see orange control loop in Fig. 3 lower panel). Otherwise, the dynamic is restricted to remain close to euthermic resting metabolic rate and body temperature, without reaching the $2 \cdot M_E$ peak detected in this previous analysis.

Hypothesis and objective of the present study

Since torpor is considered an energy conserving mechanism, it is possible that events of the exit phase can be elucidated by the study of its metabolic cost. Also, considering the ubiquity of the duration of the arousal, time spent seems to be another weighting factor in the phenomenon. Thus, because of the stereotyped nature of the dynamic observed, we hypothesized that either time or energy could be crucial variables to this phase, which appears to be regulated to allow a secure return to euthermia.

The energy savings of the torpid state were addressed long ago even taking into account the arousal phase (Wang 1979). However, a quantitative model that allows to test whether time or energy is the relevant variable at stake during this phase is not found in the literature. Then,
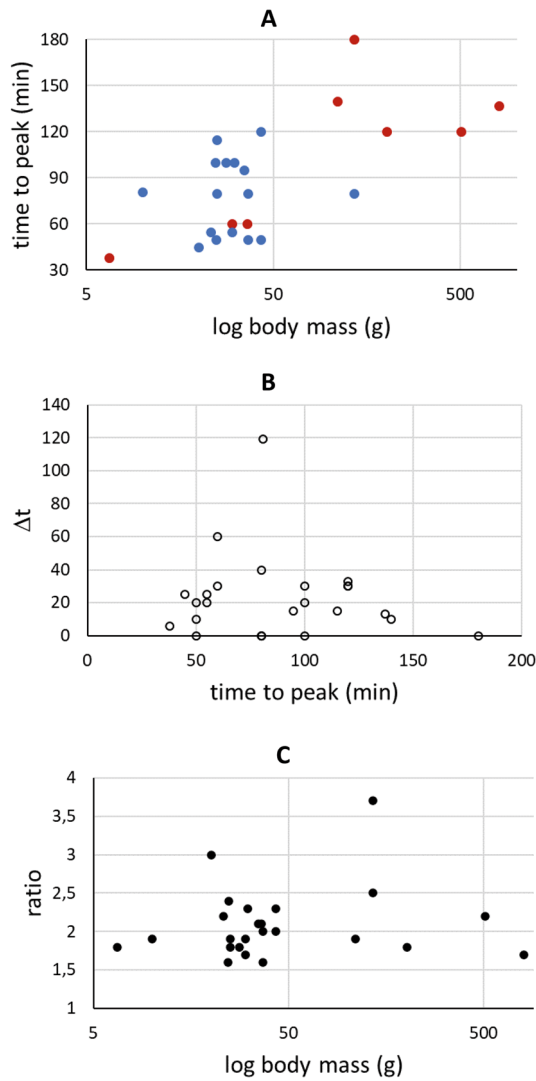
Fig. 1 A Time to metabolic peak vs log of body mass. Torpor: blue circles, hibernation: red circles. **B** Time difference (Δt) between rewarming and metabolic peak vs time to metabolic peak. **C** Ratio between metabolic peak and euthermic resting metabolic rate vs log body mass

Fig. 2 Representative scheme of the stereotyped dynamics of body temperature and metabolic rate during exit from torpor

Methods

List of symbols

c	Thermal capacitance of body fluids ($=4.12$ J g^{-1} K^{-1})	T_0	Initial body temperature at the beginning of the arousal phase
m	Body mass	T_S	Operational reference body temperature
h	Thermal conductance	k	Metabolic rate linear gain
T_B	Body temperature	α	Constant $= h^2/4 \cdot m \cdot c$
T_E	Euthermic body temperature	r	Non-dimensional gain $= k/\alpha$
T_A	Ambient temperature	γ	$\frac{h}{2 \cdot m \cdot c}$
M	Metabolic rate	Ω	$\frac{\alpha}{m \cdot c} \cdot (r-1)$
M_E	Euthermic resting metabolic rate	g	Linear gain for the setpoint temperature control system
Q	Power output (heat loss)		

Modelling

A living organism is a control volume, i.e., it exchanges energy and mass with its surroundings (e.g., (Bejan 2002)). In mammals and birds, metabolic rate is the main power input to this control volume. Specifically, during exit from

considering the oscillatory features of the arousal phase, the peak in metabolic rate and the importance of time and/or energy consumption to the organism, we constructed a model based on thermal and physiological principles that matches the currently available data to test our hypothesis. The model allows us to explain the relevance of the stereotyped dynamics in terms of optimization (in this case, minimization) of the process based on two criteria: time and energy spent.
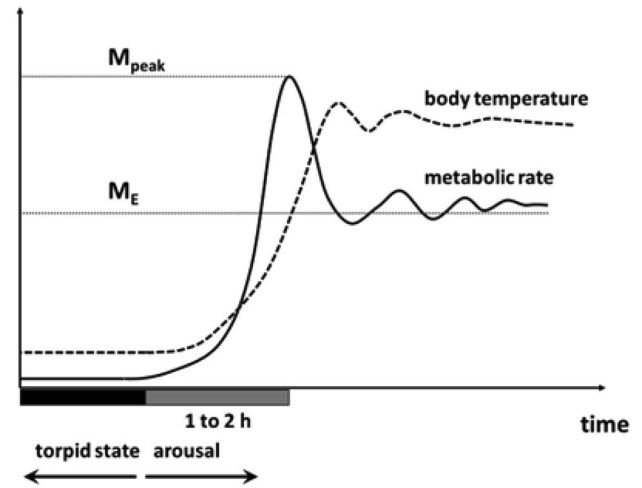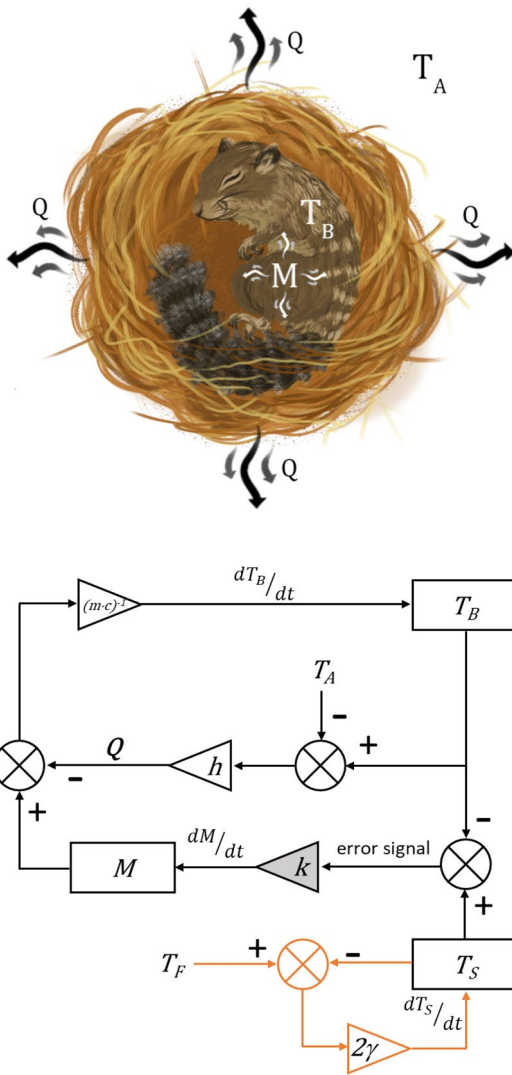
Fig. 3 Upper panel. Schematic diagram representing the power input to the system (metabolic rate, M) and its power output (heat loss to the environment, Q). The heat loss is dependent on the difference between body temperature (T_B) and ambient temperature (T_A). When there is no net change in internal energy, $Q = M$, and T_B is constant. Lower panel. Block diagram of the control system of body temperature that represents the model to be discussed and analysed in the text. Within triangles: linear gains. Within rectangles: state variables. Gray highlight: the metabolic rate gain k will be turned into a non-dimensional variable r in the development of the model and most of the conclusions will come from the analysis using this non-dimensional variable r. In orange: control loop to operate changes in the setpoint temperature during the arousal phase. This will be further presented and discussed in the text (see Eq. 35). Some lines indicate, explicitly, that the net result of the loop is a rate of change in a given state variable (particularly, M, T_B and T_S). See list of symbols for details and the description of the model in the next sections

torpor, the system is considered to exchange only heat with the environment which, then, functions as the power output. Also, any mass exchange, e.g., through breathing, is considered irrelevant to metabolism and temperature changes

which take place during the process. Any mechanical activity performed by the animal is absent or minimal due to the very nature of torpor. The temperature of the organism (T_B) is affected by the power balance between its metabolic rate (M) and heat loss (Q). The scheme in Fig. 3 summarizes the processes described above.

Basics

Metabolic rate contributes to an increase in temperature due to an increase in internal energy, while heat loss gives rise to a decrease. So, the net change in body temperature (in degrees Celsius, °C) is given by the power balance and such a balance that determines body temperature (T_B) change can be quantitatively represented as Eq. 1 (Chaui-Berlinck et al. 2005; Sunagawa and Takahashi 2016)—see Fig. 3 lower panel:

$$m \cdot c \cdot \frac{dT_B}{dt} = M - Q \qquad (1)$$

In which t, m and c are, respectively, time (in seconds), body mass (in kilograms, kg) and specific heat capacity of the organism (in joules per °C per kg); and, for the sake of notation, it is tacitly assumed that both M and Q are energy fluxes (in watts). M is a positive quantity as long as metabolic activity occurs. For an endotherm, the sign of Q is rarely positive (heat gain). T_B is the body temperature.

It was shown that heat loss is linearly proportional to the difference between body and ambient temperatures [for instance (Snapp and Heller 1981)]. Therefore, through Newton's law of cooling, the heat exchange with the environment is approximated as:

$$Q = h \cdot (T_B - T_A) \qquad (2)$$

where h is the thermal conductance (in watts per °C) and T_A is the ambient temperature.

During the entire process of exit from torpor, T_A is considered to be a constant. Total thermal conductance is considered to follow a scaling relationship with mass (Calder 1987; Schleucher and Withers 2001):

$$h = 0.005859 \cdot \sqrt{m} \qquad (3)$$

A combination of 1 and 2 gives rise to a differential equation:

$$m \cdot c \cdot \frac{dT_B}{dt} = M - h \cdot (T_B - T_A) \qquad (4)$$

Rearranging:

$$\frac{dT_B}{dt} = -\frac{h}{m \cdot c} \cdot T_B + \frac{1}{m \cdot c} \cdot M + \frac{h}{m \cdot c} \cdot T_A \qquad (5)$$

where the time dependence of T_B and M is yet to be determined.

Temperature regulation

The effect of metabolic rate on body temperature is evident by the fact that the main strategy utilized by endotherms to regulate their body temperature is by adjusting metabolic rate (Nakamura and Morrison 2008; Morrison 2018). Experimental data indicate that body temperature is regulated through a linear control of metabolic rate (e.g., Boulant 2006; Cabanac 2006; Romanovsky 2018), and see (Heller and Colliver 1974; Heller et al. 1974; Chaui-Berlinck et al. 2002, 2005) for specific modelling):

$$\frac{dM}{dt} = k \cdot (T_S - T_B) \tag{6}$$

where T_S is the operational reference body temperature for the system. There is a debate whether such a term should be setpoint, reference, or some other designation (e.g., Cabanac 2006; Romanovsky 2018)). It is not within the scope of this study to participate in this debate; thus, it will not be addressed. Even more important than do not take part in this debate are the facts that from the standpoint of control whether a reference value is a pre-set in the system or a construct of its interacting parts is not relevant and that a reference value can be changed at will.

Therefore, the terms setpoint and reference will be used interchangeably only to indicate to which temperature the system is lead to by the controller (Sunagawa and Takahashi 2016). The parameter k is the linear gain of the control system (in watts per °C per second)—it represents the intensity of change in metabolic rate given a certain deviation in body temperature from the setpoint T_S.

Treating the torpor condition as a steady state (dM/dt and dT_B/dt equal to zero), both body temperature and the operational reference are equal and at a fixed value T_0 (the initial body temperature). For the organism to exit from torpor and reach euthermia, the setpoint should increase to euthermic values, such that metabolic rate starts to increase according to Eq. 6. The following equation describes changes in T_S at the onset of exit from torpor:

$$\frac{dT_S}{dt} = g \cdot (T_E - T_S) \tag{7}$$

In which T_E is euthermic body temperature and g is the linear gain for the setpoint temperature control system (in seconds^{-1}) occurring once the organism prepares to leave the torpor condition. In other words, instead of a non-linear discontinuous step change in the temperature setpoint at a given time, Eq. 7 represents a continuous change leaving the torpid setpoint towards the euthermic

one, and the steepness of the change is given by the linear gain g. Considering the initial condition $T_S(t=0)=T_0$, the solution to this first order differential equation is given by:

$$T_S(t) = T_E - (T_E - T_0) \cdot e^{-g \cdot t} \tag{8}$$

The constant g is the inverse of the characteristic time of T_S. The characteristic time of changes in body temperature is given by the factor mc/h (see Eq. 5). If we assume g is higher than the possible values for k, then T_S reaches the euthermic value T_E faster than dM/dt reaches zero (see Eq. 6). In other words, the change in T_S from T_0 to T_E marks the beginning of the process of metabolic rate increase. Therefore:

$$T_S(t) = T_E - (T_E - T_0) \cdot e^{-\frac{h}{m \cdot c} \cdot t} \tag{9}$$

Taking into consideration this explicit equation for T_S, regulation of body temperature is represented by:

$$\frac{dM}{dt} = k \cdot \left[-T_B + T_E - (T_E - T_0) \cdot e^{-\frac{h}{m \cdot c} \cdot t} \right] \tag{10}$$

Linear control system

Next, we consider the influence of both the power balance on body temperature ($M - Q$, see Eq. 1), and its regulation through the linear control described above (see Eq. 6). Mass and thermal conductance are individual-dependent parameters and were kept constant to study the effects of the linear gain k. We can identify a constant term, $\alpha = h^2 / 4 \cdot m \cdot c$, and also define a non-dimensional variable $r = k/\alpha$ (see below). This non-dimensional variable r is directly proportional to the linear gain of the metabolic rate (Eq. 6), or, in other words, it can be interpreted as the gain in the system.

Equations 5 and 10 form an ordinary, first order, non-homogeneous system of differential equations. Through manipulation of Eq. 5 it is possible to express M in terms of T_B and its derivative:

$$M = m \cdot c \cdot \frac{dT_B}{dt} + h \cdot (T_B - T_A) \tag{11}$$

Differentiation leads to:

$$\frac{dM}{dt} = m \cdot c \cdot \frac{d^2 T_B}{dt^2} + h \cdot \frac{dT_B}{dt} \tag{12}$$

Equation 12 can be inserted into Eq. 10:

$$m \cdot c \cdot \frac{d^2 T_B}{dt^2} + h \cdot \frac{dT_B}{dt} = -k \cdot T_B + k \cdot \left[T_E - (T_E - T_0) \cdot e^{-\frac{h}{m \cdot c} \cdot t} \right] \tag{13}$$

And rearranged:

$$\frac{d^2 T_B}{dt^2} + \frac{h}{m \cdot c} \cdot \frac{dT_B}{dt} + \frac{k}{m \cdot c} \cdot T_B$$
$$= \frac{k}{m \cdot c} \cdot \left[T_E - (T_E - T_0) \cdot e^{-\frac{h}{m \cdot c} \cdot t} \right] = \frac{k}{m \cdot c} \cdot T_S \tag{14}$$

where T_S was reinserted. The solution of Eq. 14 can be split in two: the general solution to the homogeneous equation and the particular solution to the non-homogeneous one. The homogeneous solution is given by the characteristic equation:

$$\lambda^2 + \frac{h}{m \cdot c} \cdot \lambda + \frac{k}{m \cdot c} = 0 \tag{15}$$

The solution of the quadratic Eq. 15 is:

$$\lambda = -\frac{h}{2 \cdot m \cdot c} \pm \sqrt{\frac{1}{m \cdot c} \cdot \left(\frac{h^2}{4 \cdot m \cdot c} - k \right)} \tag{16}$$

We then introduce the following simplifying combinations of factors:

$$\gamma = \frac{h}{2 \cdot m \cdot c} \tag{17a}$$

$$\alpha = \frac{h^2}{4 \cdot m \cdot c} \tag{17b}$$

$$r = \frac{k}{\alpha} \tag{17c}$$

$$\Omega(r) = \frac{\alpha}{m \cdot c} \cdot (r - 1) \tag{17d}$$

After inserting Eqs. 17 into Eq. 16, the solution becomes:

$$\lambda = -\gamma \pm \sqrt{-\Omega} \tag{18}$$

The value of Ω and, thus, of r, is important to determine the behaviour of the system. The three possible solutions are $\Omega < 0$, $\Omega = 0$ and $\Omega > 0$, which translate to $r < 1$, $r = 1$ and $r > 1$, respectively. This defines three bands of the metabolic rate control system: $k < h^2/4 \cdot m \cdot c$, $k = h^2/4 \cdot m \cdot c$ and $k > h^2/4 \cdot m \cdot c$. These three bands are classically referred to as overdamped, critically damped and underdamped systems, respectively, due to the similarities to a spring–mass system. Since k is the linear gain of body temperature regulation, the solutions will be referred to match the properties of the control system: low, critical, and high gain. These three solutions will be identified by their respective values of r, a non-dimensional value that encompasses the relationship between the gain k and $h^2/4 \cdot m \cdot c$. Their functional forms for the homogeneous solutions (hom) are as follows:

$$T_B|_{\text{hom},r<1} = e^{-\gamma \cdot t} \cdot \left(C_1 \cdot e^{\sqrt{-\Omega} \cdot t} + C_2 \cdot e^{-\sqrt{-\Omega} \cdot t} \right) \tag{19}$$

$$T_B|_{\text{hom},r=1} = e^{-\gamma \cdot t} \cdot (C_1 \cdot t + C_2) \tag{20}$$

$$T_B|_{\text{hom},r>1} = e^{-\gamma \cdot t} \cdot \left[C_1 \cdot \cos\left(\sqrt{\Omega} \cdot t\right) + C_2 \cdot \sin\left(\sqrt{\Omega} \cdot t\right) \right] \tag{21}$$

The constants C_1 and C_2 are to be determined by applying initial conditions to the system of Eqs. 5 and 10 and are different for each case. A particular solution to the non-homogeneous Eq. 14 is given by $T_{B,part} = T_S$, where the subscript *part* was used to specify the particular solution. This results in the unique general solution of Eq. 14 (according to Picard's uniqueness and existence theorem):

$$T_B|_{r<1} = e^{-\gamma \cdot t} \cdot \left(C_1 \cdot e^{\sqrt{-\Omega} \cdot t} + C_2 \cdot e^{-\sqrt{-\Omega} \cdot t} \right) + T_S \tag{22}$$

$$T_B|_{r=1} = e^{-\gamma \cdot t} \cdot (C_1 \cdot t + C_2) + T_S \tag{23}$$

$$T_B|_{r>1} = e^{-\gamma \cdot t} \cdot \left[C_1 \cdot \cos\left(\sqrt{\Omega} \cdot t\right) + C_2 \cdot \sin\left(\sqrt{\Omega} \cdot t\right) \right] + T_S \tag{24}$$

The dynamic for metabolic rate is given by reintroduction of T_B into Eq. 11:

$$M|_{r<1} = m \cdot c \cdot \left[\left(\gamma + \sqrt{-\Omega} \right) \cdot C_1 \cdot e^{\left(-\gamma + \sqrt{-\Omega} \right) \cdot t} \right.$$
$$\left. + \left(\gamma - \sqrt{-\Omega} \right) \cdot C_2 \cdot e^{\left(-\gamma - \sqrt{-\Omega} \right) \cdot t} \right] + h \cdot (T_E - T_A) \tag{25}$$

$$M|_{r=1} = m \cdot c \cdot e^{-\gamma \cdot t} \cdot \left[C_1 \cdot (1 + \gamma \cdot t) + \cdot C_2 \cdot \gamma \right] + h \cdot (T_E - T_A) \tag{26}$$

$$M|_{r>1} = m \cdot c \cdot e^{-\gamma \cdot t} \left[\left(C_1 \cdot \gamma + C_2 \cdot \sqrt{\Omega} \right) \cos\left(\sqrt{\Omega} \cdot t\right) \right.$$
$$\left. + \left(C_2 \cdot \gamma - C_1 \cdot \sqrt{\Omega} \right) \sin\left(\sqrt{\Omega} \cdot t\right) \right] + h(T_E - T_A) \tag{27}$$

By recognizing that, at euthermia, the organism should have constant body temperature T_E and applying the euthermic condition to Eq. 4, euthermic resting metabolic rate M_E can be defined:

$$M_E = h \cdot (T_E - T_A) \tag{28}$$

The application of initial conditions to the three pairs of Eqs. 22/25, 23/26 and 24/27 defines the values of the constants C_1 and C_2 for each case. As described before, initial body temperature is given by T_0 and initial body temperature change, dT_B/dt, is zero. This is equivalent to affirm that initial metabolic rate, $M(t=0)$, should be given

by $h(T_0 - T_A) = M_0$. The subsequent derivation of C_1 and C_2, together with Eq. 28, results in the three complete solutions of the system. For $r < 1$:

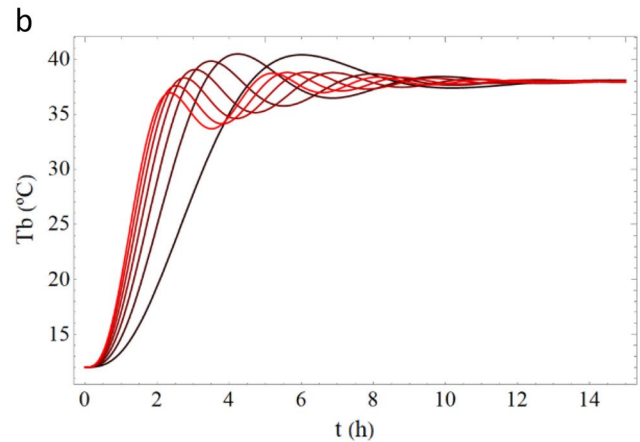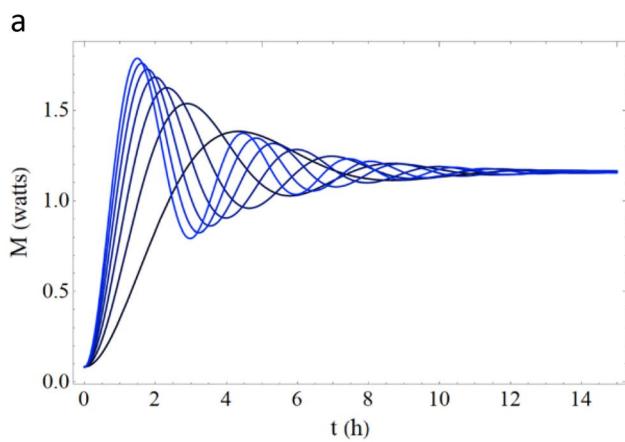$$T_B = T_S - \frac{2 \cdot \gamma}{\sqrt{-\Omega}} \cdot (T_E - T_0) \cdot e^{-\gamma \cdot t} \cdot \sinh\left(\sqrt{-\Omega} \cdot t\right) \quad (29)$$

$$M = M_E - \frac{h}{\sqrt{-\Omega}} \cdot (T_E - T_0) \cdot e^{-\gamma \cdot t} \cdot$$
$$\left[\sqrt{-\Omega} \cdot \cosh\left(\sqrt{-\Omega} \cdot t\right) + \gamma \cdot \sinh\left(\sqrt{-\Omega} \cdot t\right)\right] \quad (30)$$

For $r = 1$:

$$T_B = T_S - 2 \cdot \gamma \cdot (T_E - T_0) \cdot e^{-\gamma \cdot t} \cdot t \quad (31)$$

$$M = M_E - 2 \cdot \gamma \cdot (T_E - T_0) \cdot e^{-\gamma \cdot t} \cdot \left(\frac{h}{2} \cdot t + m \cdot c\right) \quad (32)$$

For $r > 1$:

$$T_B = T_S - \frac{2 \cdot \gamma}{\sqrt{\Omega}} \cdot (T_E - T_0) \cdot e^{-\gamma \cdot t} \cdot \sin\left(\sqrt{\Omega} \cdot t\right) \quad (33)$$

Fig. 4 Dynamics for metabolic rate (**a**) and body temperature (**b**) over time during the exit from torpor for seven different values of the parameter r ranging from 5, darker blue/red, to 35, brighter blue/red, in steps of 5. Note that metabolic rate and body temperature present damped oscillations around their euthermic values
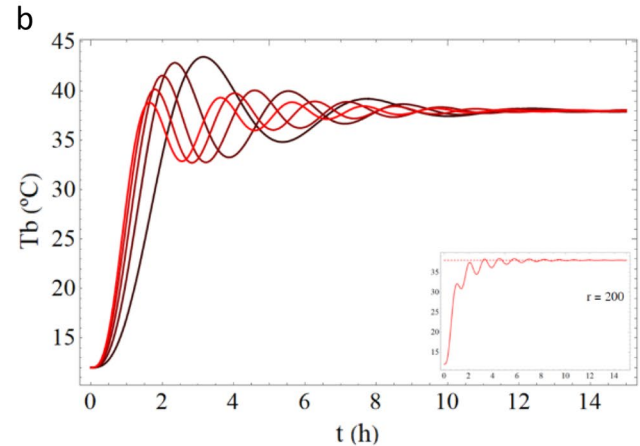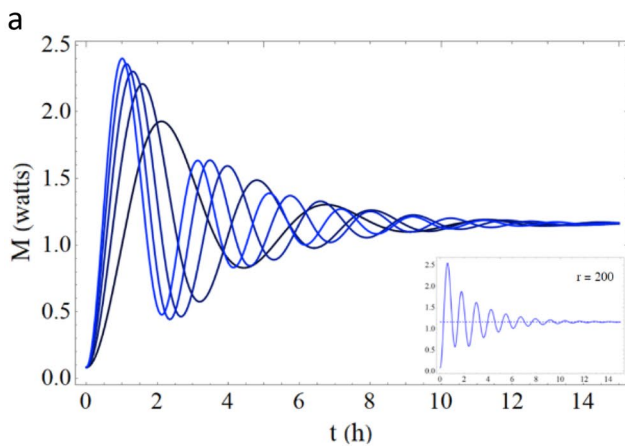

Fig. 5 Dynamics of metabolic rate (**a**) and body temperature (**b**) over time during the exit from torpor for five different values of the parameter r, from 15, darker blue/red, to 75, brighter blue/red, in steps of 15, with upregulation of the body temperature setpoint. In the insets, the dynamics for $r = 200$ are shown. Notice that dynamics with higher values of r asymptotically tend to a peak slightly above $2 \cdot Me$ (see Appendix)

$$M = M_E - \frac{h}{\sqrt{\Omega}} \cdot (T_E - T_0) \cdot e^{-\gamma \cdot t}.$$
$$\left[\sqrt{\Omega} \cdot \cos\left(\sqrt{\Omega} \cdot t \right) + \gamma \cdot \sin\left(\sqrt{\Omega} \cdot t \right) \right] \quad (34)$$

The dynamics for $r > 1$ behave similarly to the experimental data currently available (see Figs. 1, 4 and 5), where both the damped oscillations and a distinct peak of metabolic rate are observed.

Results

General dynamics

Figure 4 shows the time course given by Eqs. 33 and 34 for different values of $r > 1$ (see caption). The numerical values of the parameters body mass, specific heat capacity, thermal conductance, euthermic body temperature and ambient temperature are specified in the Appendix—Upregulation of T_s.

At this point, we have the mathematical framework for the exit from torpor. However, the $2 \cdot M_E$ peak is not yet achieved. Therefore, as anticipated, there should be a period of fast changes in T_S towards the euthermic value. This can be accomplished by an upregulation of T_S (see Appendix and Fig. 3 lower panel in orange). In fact, this resembles a mirror image of the entry phase where Sunagawa & Takahashi have shown a reduction in the sensitivity (i.e., gain) of the thermo-control system (Sunagawa and Takahashi 2016).

Given the timeframe of exit from torpor, a mean value of 1.5 h was chosen as the period of upregulation, in which the aimed value is 45 °C. This is also consistent with the 60 min time-frame of changes in hypercapnic ventilatory response observed in the arousal from hibernation in 13-lined ground
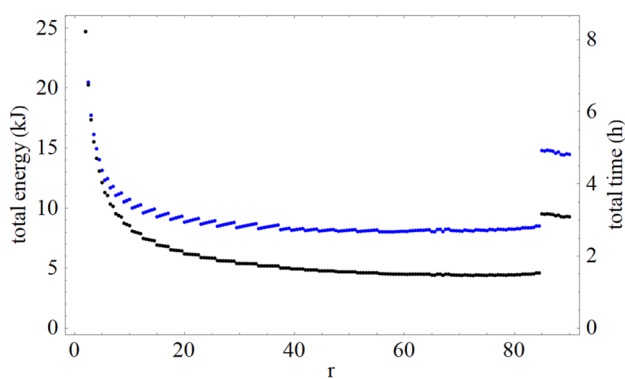
Table 2 Time and energy spent in the exit from torpor as a function of r

r	Time spent (h)	Energy spent (kJ)
72.5	**1.46**	8.10
58.0	1.50	**8.03**
65.5	1.47	8.04

The minimal values are highlighted in bold

squirrels (*Ictidomys tridecemlineatus*—(Sprenger and Milsom 2022)).

The time course of Eqs. 33 and 34 with the upregulation in T_S can be seen in Fig. 5 for different values of r. The metabolic peak of approximately $2 \cdot M_E$ is now obtained. It is important to note that, even though the aimed value for the setpoint is 45 °C, the actual body temperature is kept within the physiological range.

What is left to tackle in this study is a relationship between these different values of r and the hypothesized optimization of either time and/or energy spent. This is shown in Fig. 6, that contain the total time and energy spent during exit from torpor—up to the point when Tb reaches T_E for the first time—for different r values.

The minimum in each plot was determined to be at $r = 72.5$ for time and $r = 58$ for energy spent. The minimal values are shown in Table 2, together with an intermediate value of r, 65.5. As it can be clearly observed, there is little to no variation in time and energy spent within this range of r. In other words, the exact value of r is irrelevant to the minimization of both these quantities, as long as the control system of the organism remains close to these high r values. The choice of 65.5, although arbitrary, illustrates this. Figure 7 shows how metabolic rate and body temperature behave according to this value. Both the total energy and
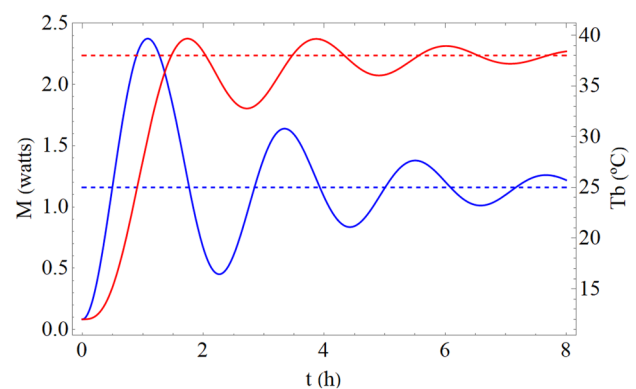

Fig. 6 Total time (black) and total energy (blue) spent during exit from torpor for different values of r (from 2 to 90, in steps of 0.5). The minimal time spent, 1.46 h, was achieved at $r = 72.5$. The minimal energy spent, 8.03 kJ, was achieved at $r = 58.0$. The discontinuity at around $r = 85$ is explained in the Appendix

Fig. 7 Illustrative plot of metabolic rate and body temperature during exit from torpor, simulated for a 50 g animal with $r = 65.5$. Metabolic rate in blue, body temperature in red
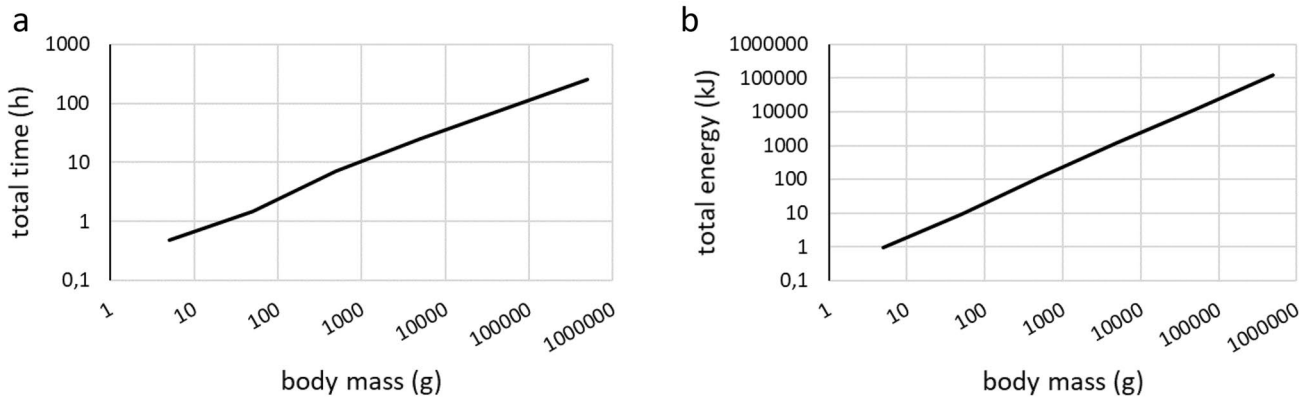
Fig. 8 Minimal total time (**a**) and minimal total energy (**b**) spent during exit from torpor as a function of body mass (log–log). The values of body mass range from 5 g to 500 kg
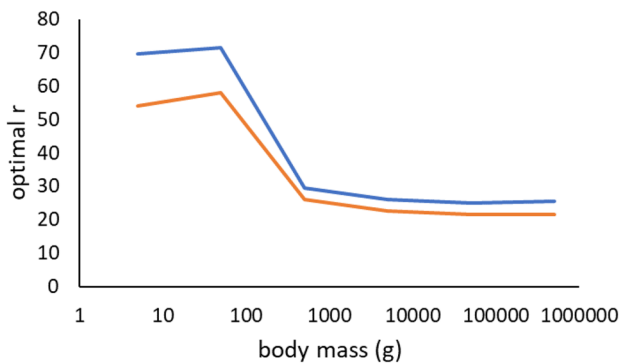

Fig. 9 Optimal r for total time (in blue) and energy (in orange) as a function of body mass (semi-log). The values of body mass range from 5 g to 500 kg. Notice the discrete change in optimal r between 50 and 500 g

total time spent are close to the minimum and the $2 \cdot M_E$ peak is achieved, giving rise to a dynamic quite similar to the one presented in Fig. 1.

Scaling

A broader application of our model was tested to understand how body mass affects the minimal values of time and energy spent, and also the values of r that satisfy these minima. Figures 8 and 9 show how these relations hold. Minimal time spent scales with an exponent of 0.55, while minimal energy, with 1.03. In other words, time scales approximately with the square root of body mass and energy is linear with body mass, with an inclination of 0.25 kJ/g. On the other hand, r values do not show a simple scaling rule, and, in fact, have an optimum value
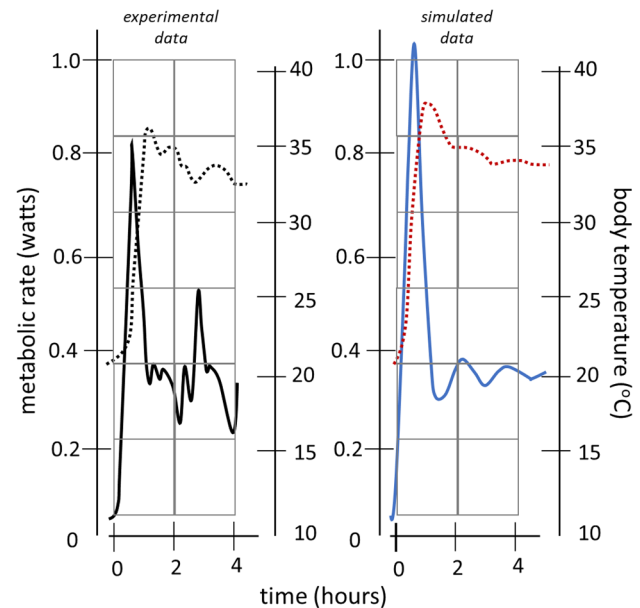

Fig. 10 Dynamics of body temperature and metabolic rate during arousal in real data from *Sminthopsis macroura* (left hand panel—metabolic rate in solid black and body temperature in dotted black) and according to the model (right hand panel—metabolic rate in solid blue, body temperature in dotted red). $r = 65.5$, $T_G = T_E + 7$, $\tau = 1.5$ h. The x-axis scale was kept similar to the original (experimental) data presentation. Body mass of 25 g and ambient temperature of 19 °C (Geiser et al. 1996)

of around 65 for body mass below 100 g, and around 25 for body mass above 100 g (see Fig. 9). It is important to keep in mind that there are no confirmed examples of true torpor in large mammals (e.g., (Heldmaier et al. 2004)), and, therefore, the scaling of the thermal conductance is more adequate for small animals.

Comparing the model to real data of daily torpor

The model was applied to a mammal of 25 g (*Sminthopsis macroura*) exiting daily torpor (Geiser et al. 1996). The parameters of the simulation were $T_A = 19$, $T_E = 34$ and $T_0 = 21$, as in the original experiment. Figure 10 shows the comparison between real data and the model—notice the striking resemblance between them.

Discussion

Initially, it is important to note that the aim of the present study was neither to address any specific case nor to make any model fitting to particular events. Our goal was to consider a general problem—the somewhat stereotyped dynamics of the arousal from the torpid state—and use minimal information to address the issue of whether this stereotyped dynamic optimize the transition to the euthermic condition. We hypothesized that minimization in time or in energy consumption might underlie this metabolic behaviour and addressed the issue building a mathematical framework.

The model was constructed from a collection of first principles of physiology, control engineering and thermodynamics, namely: the power balance between metabolic rate and heat exchange, and endothermic body temperature control system. Moreover, the model is quite parsimonious: it is based on only three coupled linear differential equations (eqs. 1, 6 and 7). When we applied these principles to the torpor arousal phase, the model produced patterns in both body temperature and metabolic rate dynamics that reproduce real data accurately (compare Figs. 1 and 7 and see Fig. 10).

During torpor, an animal is subjected to physiological conditions that might jeopardize survival, as the low macromolecular turnover and cellular repairing rates (Storey 2010), thermal stress associated to energy depletion or other oxidative stressors (Carey et al. 1999, 2000). In fact, the arousal phase, due to the increased oxygen demand, might impose risks for its own (Lee et al. 2002; Storey 2010). In this sense, it is ample documented the use of the so-called cold arousals in bats during hibernation (Bartonička et al. 2017; Mayberry et al. 2018). These cold arousals are slight elevations in body temperature without completing the return to euthermia and seem to fulfil a yet unknown role. Besides cold arousals, hibernating animals might present the so-called alarm arousals, which are a complete return to euthermic conditions due to external perturbations (Utz and van Breukelen 2013) and follow a similar time pattern as the natural ones. Therefore, the full arousal is also expected to preserve the integrity of the organism in the best possible way.

Given that torpor is thought to be an energy-preserving mechanism, it makes sense that the energy spent should be minimized during the whole process, including its exit. Moreover, before they get access to food after arousal, most of the hibernators and daily torpids shall become active (Hume et al. 2002; Cotton and Harlow 2010; Tøien et al. 2011; Gao et al. 2012; Hindle et al. 2015) and, thus, need their energy storages to not be completely exhausted (Dausmann and Warnecke 2016; Bartsiokas and Arsuaga 2020).

The model shows that the stereotyped pattern of exit from torpor is in fact a double solution: it saves time and preserves energy storages. In other words, even though our primary hypotheses were a minimization in either time or energy, we found that it is possible for the controller to simultaneously minimize both (see Table 2).

Figure 6 shows that there is a given range of r, approximately between 58 and 72.5, for which there is little to no variation in both the time and the energy spent during exit from torpor. This parameter r is a measure of the intensity of the linear gain of the control system of body temperature. Therefore, the higher the value of r, the greater the acceleration of metabolic rate responses. The opposite is true for low values of r, which imply a slow response in metabolism.

The fall in body temperature during the entry phase is accounted for by a decrease in the hypothalamic setpoint (Heller and Kilduff 1985) and changes related to the autonomic nervous system (i.e., heart and respiratory rates, cerebral blood flow and oxygen consumption) lead changes in body temperature (Drew et al. 2007). The rise in body temperature and metabolic rate during exit from torpor is credited to a rise in the hypothalamic setpoint (Sunagawa and Takahashi 2016). Therefore, similar to the entrance phase, changes in metabolic rate precede changes in body temperature. The current view regarding the activation of heat production in the arousal from torpor holds that it is a sympathetically driven process (Braulke and Heldmaier 2010; Nedergaard and Cannon 2018; Shi et al. 2021)). This increase in sympathetic activity might explain both the increase in heat production and the overshoot in the temperature setpoint. In this sense of sympathetic activation, it was observed that systolic blood pressure has an overshoot that precedes body temperature peak (similar to what happens to metabolic rate) during the arousal phase from hibernation in Syrian hamsters (Horwitz et al. 2013), indicating, as in the case of the hypercapnic ventilatory response cited earlier, that the references in the controllers are in change during this phase. The termination in the setpoint overshoot is probably due to the rise in body temperature itself which would close a loop in another control layer. This investigation is left to other studies.

From a slight different perspective, the alarm arousals cited earlier show an interesting point: body temperature increases at a faster rate than in natural arousals (Utz and van

Breukelen 2013). This fact, as the authors conclude, might indicate that natural arousals are controlled to occur at a slower pace than the maximum possible for the animal. This observation reinforces our present analysis: the stereotyped time-profile of natural arousals is a controlled process to minimize both time and energy during the exit from torpor.

Thus, we conjecture that the exit from torpor occurs by obeying the following events:

1. once the arousal is triggered in the central nervous system, during a brief period of time (e.g., 1 h) the setpoint is overshot to a value above the euthermic temperature;
2. this causes a huge acceleration in metabolic rate according to the gain in the control system;
3. then, body temperature starts to rise in an accelerated way as well;
4. after that brief period of time the setpoint is set to the euthermic value and metabolic rate and body temperature tend to damped oscillations around their respective euthermic values.

The importance of the gain in the control system lies in the amount of time and energy spent during this arousal process. Experimental data evidence that small hibernators mammals have, indeed, a higher gain in their temperature control system than larger non-hibernating ones (Heller et al. 1974), and, also, that such a gain is higher in euthermia than in the torpid state (Sunagawa and Takahashi 2016), as predict by the model.

Our modelling implies that large mammals are restricted in the use of torpor due to the optimal values of the linear gain in temperature regulation, around $r = 25$. These values, combined with the setpoint parameters τ and T_G (see Appendix), do not allow a metabolic peak of $2 \cdot M_E$ (simulations not shown). Clearly, there are many factors involved in the restriction of metabolic depression in large endotherms other than the optimality in the arousal phase which are beyond the present modelling.

Large mammals are observed to hibernate with only a small drop in T_B and a slow exit profile (Tøien et al. 2011; Choukèr et al. 2019), without the metabolic peak characteristic of torpor. This suggests a metabolic restriction in the arousal, as indicated by our model. In this sense, as proposed by other authors, body temperature should not be the criterion to define hibernation (Dausmann et al. 2005). From the present study, we suggest that this ratio between M_{peak} and M_E could be employed to distinguish among depressed metabolic states.

Temperature effects on metabolic rate is a highly debatable issue. Many understand it as a causative factor: body temperature itself causes the metabolic rate attained. Some understand it as a permissive factor: the increase in body temperature allows for an increase in chemical reaction rates (Chaui-Berlinck et al. 2004). The former, usually cited as "Q_{10} effect", is incompatible with metabolic control of thermoregulation while the latter does not interfere with thermoregulation via metabolic control. The problem is that which view of "temperature effects" the authors are considering is seldom made explicit in the reports.

While there is an equivocal debate regarding temperature effects on metabolic rate, viz "Q_{10} effects", in the entry phase (Snyder and Nestler 1990; Heldmaier and Ruf 1992; Heldmaier et al. 1999, 2004; Ortmann and Heldmaier 2000; Nogueira de Sá and Chaui-Berlinck 2022), the arousal was never truly credited to these effects. Utz and collaborators (Utz et al. 2007) made an attempt to input the increase in metabolic rate to temperature effects (Q_{10} effects) during the exit phase and verified, as the authors state, "the curious fact" that the arousing animals show a decrease in their rates of rewarming around the middle of the process even though body temperature continues to rise, and clearly this cannot be explained through temperature effects on metabolic rate. Our model clarifies this because there are no causative temperature effects on metabolic rate at all, and the "curious fact" highlights the control system at full action, indeed. Clearly, this does not preclude temperature as a permissive effect.

Appendix

Upregulation of T_s

The graphical visualization of the dynamics of M and T_B, determined by Eqs. 29 through 34, requires that numerical values are assigned to all constants. The organism is considered to have body mass $m = 50$ g, specific heat capacity $c = 4.12$ J/°C·gram (Haemmerich et al. 2005),
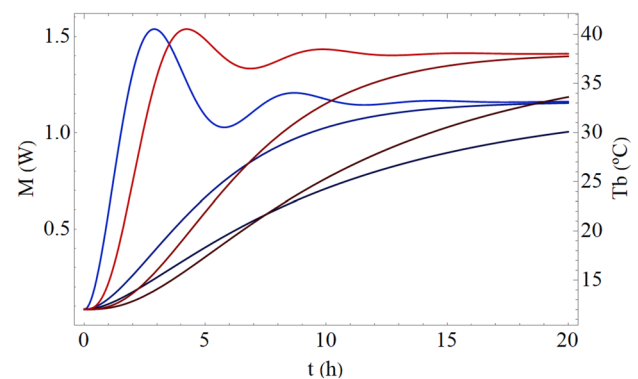
Fig. 11 Examples of dynamics of metabolic rate (blue lines) and body temperature (red lines) along the time (in hours) accordingly to equations from 29 to 34. Darker colours represent low gain ($r = 0.5$), intermediate colours represent critical gain ($r = 1$) and lighter colours represent high gain ($r = 10$)
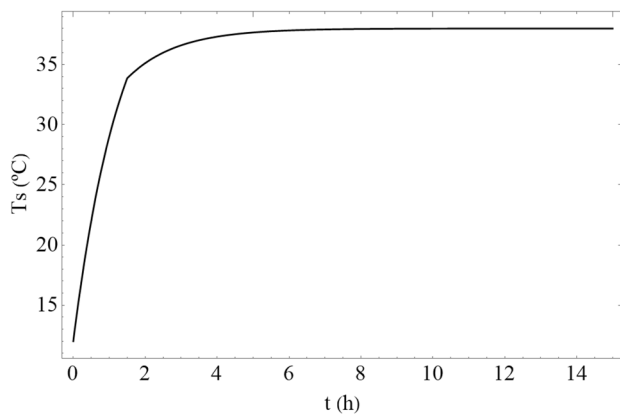
Fig. 12 Dynamic for T_S (in °C) as a function of time (in hours), according to Eq. 35. Notice that at 1.5 h there is a change in the behaviour of the dynamic due to the change in T_F (Eq. 36). It is important to highlight that this dynamic does not depend on the values of T_B, M or r

euthermic body temperature $T_E = 38$ °C and initial temperature $T_0 = 12$ °C. Considering Eq. 3 and a mass of 50 g, total thermal conductance (h) has a value of 0.001310 watts/°C (0.22 mL O_2 h^{-1} °C^{-1}). The environment is considered to be at constant temperature $T_A = 10$ °C. These values result in an euthermic resting metabolic rate $M_E = 1.16$ watts and an initial metabolic rate $M_0 = 0.083$ watts, independently of the gain k. For the sake of comparison, the elephant shrew *Elephantulus rozeti* with body mass of 45 g at T_A of 10 °C has an euthermic oxygen consumption rate of 5 mL O_2 g^{-1} h^{-1} which results in 1.26 watts (Lovegrove et al. 2001).

The time course of metabolic rate and body temperature described by Eqs. 34–39 are plotted in Fig. 11. Note that the brighter lines, which represent the high gain case, have dynamics that resemble the stereotyped behaviour of exit from torpor shown in Fig. 1. Therefore, in the remaining of the analysis, we focus only on values of r greater than 1.

As explained in the main text, we have the mathematical framework for the general behaviour of the exit from torpor, nevertheless, without the $2 \cdot M_E$ peak. This can be accomplished by an upregulation of T_S. To implement the change in the setpoint during the process of exit, Eq. 7 was changed to:

$$\frac{dT_S}{dt} = 2 \cdot \gamma \cdot \left(T_F(t) - T_S \right) \tag{35}$$

where $T_F(t)$ is given by:

$$T_F(t) = T_G + \left(T_G - T_E \right) \cdot \left(e^{-2 \cdot \gamma \cdot (t - \tau)} - 1 \right) \cdot \theta(t - \tau) \tag{36}$$

T_G is a value which the setpoint would try to achieve before aiming for T_E, τ is the time at which the setpoint dynamic would change and $\theta(t)$ is the Heaviside Step Function. Equation 36 describes a function which has

constant value T_G until time τ, after which there is a step change to $T_F(t > \tau) = T_E$. Considering the same 50 g organism described before, we have $T_G = T_E + 7$ °C (in this case, 45 °C) and $\tau = 5,400$ s (1.5 h). New equations for T_S, T_B and M were obtained through the following system:

$$\frac{dT_B}{dt} = -\frac{h}{m \cdot c} \cdot T_B + \frac{1}{m \cdot c} \cdot M + \frac{h}{m \cdot c} \cdot T_A \tag{37}$$

$$\frac{dM}{dt} = k \cdot (T_S - T_B) \tag{38}$$

$$\frac{dT_S}{dt} = 2 \cdot \gamma \cdot \left(T_F(t) - T_S \right) \tag{39}$$

Numerical integrations were done for T_S, M and T_B—the unique dynamic for T_S is shown in Fig. 12, while some dynamics for M and T_B, which depend on r, are shown in Fig. 5 of the main text.

Calculations of the total time and energy spent during the process were done for different values of r. Total time was defined as the time at which T_B reaches and crosses T_E for the first time (after that, it starts to oscillate around T_E). The total energy spent was the integral of $M(t)$ from time zero to that total time. Figures 6 and 7 show these results (see main text).

For different values of r, T_B will cross T_E at different phases of the oscillation, giving rise to the discontinuity seen in Figs. 6 and 7, at around $r = 85$. The insets in Fig. 5 illustrate this.

References

Bartonička T, Bandouchova H, Berková H et al (2017) Deeply torpid bats can change position without elevation of body temperature. J Therm Biol 63:119–123. https://doi.org/10.1016/j.jtherbio.2016.12.005

Bartsiokas A, Arsuaga JL (2020) Hibernation in hominins from Atapuerca, Spain half a million years ago. Anthropol 124:102797. https://doi.org/10.1016/j.anthro.2020.102797

Bejan A (2002) Fundamentals of exergy analysis, entropy generation minimization, and the generation of flow architecture. Int J Energy Res 26:545–565. https://doi.org/10.1002/er.804

Boulant JA (2006) Neuronal basis of Hammel's model for set-point thermoregulation. J Appl Physiol 100:1347–1354. https://doi.org/10.1152/japplphysiol.01064.2005

Braulke LJ, Heldmaier G (2010) Torpor and ultradian rhythms require an intact signalling of the sympathetic nervous system. Cryobiology 60:198–203. https://doi.org/10.1016/j.cryobiol.2009.11.001

Brown JCL, Gerson AR, Staples JF (2007) Mitochondrial metabolism during daily torpor in the dwarf Siberian hamster: role of active

regulated changes and passive thermal effects. Am J Physiol Regul Integr Comp Physiol. https://doi.org/10.1152/ajpregu.00310.2007

Cabanac M (2006) Adjustable set point: to honor Harold T. Hammel J Appl Physiol 100:1338–1346. https://doi.org/10.1152/japplphysiol.01021.2005

Calder WA (1987) Scaling energetics of homeothermic vertebrates: an operational allometry. Annu Rev Physiol 49:107–120. https://doi.org/10.1146/annurev.ph.49.030187.000543

Carey HV, Sills NS, Gorham DA (1999) Stress proteins in mammalian hibernation. Am Zool 39:825–835. https://doi.org/10.1093/icb/39.6.825

Carey HV, Frank CL, Seifert JP (2000) Hibernation induces oxidative stress and activation of NF-κB in ground squirrel intestine. J Comp Physiol B Biochem Syst Environ Physiol 170:551–559. https://doi.org/10.1007/s003600000135

Chaui-Berlinck JG, Alves Monteiro LH, Navas CA, Bicudo JEPW (2002) Temperature effects on energy metabolism: a dynamic system analysis. Proc R Soc London Ser B Biol Sci 269:15–19. https://doi.org/10.1098/rspb.2001.1845

Chaui-Berlinck JG, Navas CA, Alves Monteiro LH, Pereira Wilken Bicudo JE (2004) Temperature effects on a whole metabolic reaction cannot be inferred from its components. Proc R Soc B Biol Sci 271:1415–1419. https://doi.org/10.1098/rspb.2004.2727

Chaui-Berlinck JG, Navas CA, Monteiro LHA, Bicudo JEPW (2005) Control of metabolic rate is a hidden variable in the allometric scaling of homeotherms. J Exp Biol 208:1709–1716. https://doi.org/10.1242/jeb.01421

Cheng CL (2008) Is human hibernation possible? Annu Rev Med 59:177–186. https://doi.org/10.1146/annurev.med.59.061506.110403

Choukèr A, Bereiter-hahn J, Singer D, Heldmaier G (2019) Hibernating astronauts—science or fiction? Pflügers Arch 471:819–828

Cotton CJ, Harlow HJ (2010) Avoidance of skeletal muscle atrophy in spontaneous and facultative hibernators. Physiol Biochem Zool 83:551–560. https://doi.org/10.1086/650471

Dausmann KH, Warnecke L (2016) Primate torpor expression: ghost of the climatic past. Physiology 31:398–408. https://doi.org/10.1152/physiol.00050.2015

Dausmann KH, Glos J, Ganzhorn JU, Heldmaier G (2005) Hibernation in the tropics: lessons from a primate. J Comp Physiol B Biochem Syst Environ Physiol 175:147–155. https://doi.org/10.1007/s00360-004-0470-0

Drew KL, Buck CL, Barnes BM et al (2007) Central nervous system regulation of mammalian hibernation: implications for metabolic suppression and ischemia tolerance. J Neurochem 102:1713–1726. https://doi.org/10.1111/j.1471-4159.2007.04675.x

Gao Y-F, Wang J, Wang H-P et al (2012) Skeletal muscle is protected from disuse in hibernating dauria ground squirrels. Comp Biochem Physiol Part A Mol Integr Physiol 161:296–300. https://doi.org/10.1016/j.cbpa.2011.11.009

Geiser F (2004) Metabolic rate and body temperature reduction during hibernation and daily torpor. Annu Rev Physiol 66:239–274. https://doi.org/10.1146/annurev.physiol.66.032102.115105

Geiser F, Song X, Körtner G (1996) The effect of He-O2 exposure on metabolic rate, thermoregulation and thermal conductance during normothermia and daily torpor. J Comp Physiol B Biochem Syst Environ Physiol 166:190–196. https://doi.org/10.1007/BF00263982

Geiser F, Kortner G, Schmidt I (1998) Leptin increases energy expenditure of a marsupial by inhibition of daily torpor. Am J Physiol Integr Comp Physiol 275:1627–1632

Geiser F, Currie SE, O'Shea KA, Hiebert SM (2014) Torpor and hypothermia: reversed hysteresis of metabolic rate and body temperature. Am J Physiol Integr Comp Physiol 307:R1324–R1329. https://doi.org/10.1152/ajpregu.00214.2014

Geiser F, Stawski C, Wacker CB, Nowack J (2017) Phoenix from the ashes: fire, torpor, and the evolution of mammalian endothermy. Front Physiol 8

Haemmerich D, Schutt DJ, Dos Santos I et al (2005) Measurement of temperature-dependent specific heat of biological tissues. Physiol Meas 26:59–67. https://doi.org/10.1088/0967-3334/26/1/006

Hammel HT, Dawson TJ, Abrams RM, Andersen HT (1968) Total calorimetric measurements on citellus lateralis in hibernation. Physiol Zool 41:341–357. https://doi.org/10.1086/physzool.41.3.30155466

Heldmaier G, Ruf T (1992) Body temperature and metabolic rate during natural hypothermia in endotherms. J Comp Physiol B 162:696–706. https://doi.org/10.1007/BF00301619

Heldmaier G, Klingenspor M, Werneyer M et al (1999) Metabolic adjustments during daily torpor in the Djungarian hamster. Am J Physiol Endocrinol Metab. https://doi.org/10.1152/ajpendo.1999.276.5.e896

Heldmaier G, Ortmann S, Elvert R (2004) Natural hypometabolism during hibernation and daily torpor in mammals. Respir Physiol Neurobiol 141:317–329. https://doi.org/10.1016/j.resp.2004.03.014

Heller H, Colliver G (1974) CNS regulation of body temperature during hibernation. Am J Physiol Content 227:583–589. https://doi.org/10.1152/ajplegacy.1974.227.3.583

Heller HC, Kilduff TS (1985) Neural control of mammalian hibernation. In: Gilles R (ed) Circulation, respiration, and metabolism. Springer, Berlin Heidelberg, Berlin, Heidelberg, pp 519–530

Heller H, Colliver G, Anand P (1974) CNS regulation of body temperature in euthermic hibernators. Am J Physiol Content 227:576–582. https://doi.org/10.1152/ajplegacy.1974.227.3.576

Hindle AG, Otis JP, Elaine Epperson L et al (2015) Prioritization of skeletal muscle growth for emergence from hibernation. J Exp Biol 218:276–284. https://doi.org/10.1242/jeb.109512

Horwitz BA, Chau SM, Hamilton JS et al (2013) Temporal relationships of blood pressure, heart rate, baroreflex function, and body temperature change over a hibernation bout in Syrian hamsters. Am J Physiol Regul Integr Comp Physiol 305:759–768. https://doi.org/10.1152/ajpregu.00450.2012

Hume I, Beiglbock C, Ruf T et al (2002) Seasonal changes in morphology and function of the gastrointestinal tract of free-living alpine marmots (Marmota marmota). J Comp Physiol B 172:197–207. https://doi.org/10.1007/s00360-001-0240-1

Karpovich SA, Tøien Ø, Buck CL, Barnes BM (2009) Energetics of arousal episodes in hibernating arctic ground squirrels. J Comp Physiol B Biochem Syst Environ Physiol 179:691–700. https://doi.org/10.1007/s00360-009-0350-8

Kelm DH, Von Helversen O (2007) How to budget metabolic energy: torpor in a small Neotropical mammal. J Comp Physiol B Biochem Syst Environ Physiol 177:667–677. https://doi.org/10.1007/s00360-007-0164-5

Lee M, Choi I, Park K (2002) Activation of stress signaling molecules in bat brain during arousal from hibernation. J Neurochem 82:867–873. https://doi.org/10.1046/j.1471-4159.2002.01022.x

Lovegrove BG, Raman J, Perrin MR (2001) Heterothermy in elephant shrews, Elephantulus spp. (Macroscelidea): daily torpor or hibernation? J Comp Physiol B 171:1–10

Mayberry HW, McGuire LP, Willis CKR (2018) Body temperatures of hibernating little brown bats reveal pronounced behavioural activity during deep torpor and suggest a fever response during white-nose syndrome. J Comp Physiol B 188:333–343. https://doi.org/10.1007/s00360-017-1119-0

Mohr SM, Bagriantsev SN, Gracheva EO (2020) Cellular, molecular, and physiological adaptations of hibernation: the solution to environmental challenges. Annu Rev Cell Dev Biol 36:315–338. https://doi.org/10.1146/annurev-cellbio-012820-095945

Morrison SF (2018) Efferent neural pathways for the control of brown adipose tissue thermogenesis and shivering, 1st edn. Elsevier B.V

Nakamura K, Morrison SF (2008) A thermosensory pathway that controls body temperature. Nat Neurosci 11:62–71. https://doi.org/10.1038/nn2027

Nedergaard J, Cannon B (2018) Brown adipose tissue as a heat-producing thermoeffector, 1st edn. Elsevier B.V

Nogueira de Sá PG, Chaui-Berlinck JG (2022) A thermodynamic-based approach to model the entry into metabolic depression by mammals and birds. J Comp Physiol B 192:593–610. https://doi.org/10.1007/s00360-022-01442-9

Ortmann S, Heldmaier G (2000) Regulation of body temperature and energy requirements of hibernating Alpine marmots (Marmota marmota). Am J Physiol Integr Comp Physiol 278:R698–R704. https://doi.org/10.1152/ajpregu.2000.278.3.R698

Romanovsky AA (2018) The thermoregulation system and how it works, 1st edn. Elsevier B.V

Ruf T, Geiser F (2015) Daily torpor and hibernation in birds and mammals. Biol Rev 90:891–926. https://doi.org/10.1111/brv.12137

Ruf T, Heldmaier G (1992) The impact of daily torpor on energy requirements in the Djungarian Hamster, Phodopus sungorus. Physiol Zool 65:994–1010. https://doi.org/10.1086/physzool.65.5.30158554

Ruf T, Gasch K, Stalder G et al (2021) An hourglass mechanism controls torpor bout length in hibernating garden dormice. J Exp Biol. https://doi.org/10.1242/jeb.243456

Schleucher E, Withers PC (2001) Re-evaluation of the allometry of wet thermal conductance for birds. Comp Biochem Physiol A Mol Integr Physiol 129:821–827

Shi Z, Qin M, Huang L et al (2021) Human torpor: translating insights from nature into manned deep space expedition. Biol Rev 96:642–672. https://doi.org/10.1111/brv.12671

Snapp BD, Heller HC (1981) Suppression of metabolism during hibernation in Ground Squirrels (Citellus lateralis). Physiol Zool 54:297–307. https://doi.org/10.1086/physzool.54.3.30159944

Snyder GK, Nestler JR (1990) Relationships between body temperature, thermal conductance, Q10 and energy metabolism during daily torpor and hibernation in rodents. J Comp Physiol B 159:667–675. https://doi.org/10.1007/BF00691712

Song X, Kortner G, Geiser F (1995) Reduction of metabolic rate and thermoregulation during daily torpor. J Comp Physiol B 165:291–297. https://doi.org/10.1007/BF00367312

Song X, Körtner G, Geiser F (1997) Thermal relations of metabolic rate reduction in a hibernating marsupial. Am J Physiol Regul Integr Comp Physiol 273:2097–2104. https://doi.org/10.1152/ajpregu.1997.273.6.r2097

Sprenger RJ, Milsom WK (2022) Changes in CO2 sensitivity during entrance into, and arousal from hibernation in Ictidomys tridecemlineatus. J Comp Physiol B Biochem Syst Environ Physiol 192:361–378. https://doi.org/10.1007/s00360-021-01418-1

Staples JF (2016) Metabolic flexibility: hibernation, torpor, and estivation. Compr Physiol 6:737–771. https://doi.org/10.1002/cphy.c140064

Storey KB (2010) Out cold: biochemical regulation of mammalian hibernation—a mini-review. Gerontology 56:220–230. https://doi.org/10.1159/000228829

Sunagawa GA, Takahashi M (2016) Hypometabolism during daily torpor in mice is dominated by reduction in the sensitivity of the thermoregulatory system. Sci Rep 6:1–14. https://doi.org/10.1038/srep37011

Swoap SJ (2008) The pharmacology and molecular mechanisms underlying temperature regulation and torpor. Biochem Pharmacol 76:817–824. https://doi.org/10.1016/j.bcp.2008.06.017

Thomas DW, Dorais M, Bergeron J-M (1990) Winter energy budgets and cost of arousals for hibernating little brown bats, Myotis lucifugus. J Mammal 71:475–479

Tøien Ø, Blake J, Edgar DM et al (2011) Hibernation in black bears: suppression from body temperature. Science 331:906–909

Utz JC, van Breukelen F (2013) Prematurely induced arousal from hibernation alters key aspects of warming in golden-mantled ground squirrels, Callospermophilus lateralis. J Therm Biol 38:570–575. https://doi.org/10.1016/j.jtherbio.2013.10.001

Utz JC, Velickovska V, Shmereva A, van Breukelen F (2007) Temporal and temperature effects on the maximum rate of rewarming from hibernation. J Therm Biol 32:276–281. https://doi.org/10.1016/j.jtherbio.2007.02.002

Wang LCH (1979) Time patterns and metabolic rates of natural torpor in the Richardson's ground squirrel. Can J Zool 57:149–155. https://doi.org/10.1139/z79-012

Wang LCH, Wolowyk MW (1988) Torpor in mammals and birds. Can J Zool 66:133–137. https://doi.org/10.1139/z88-017

Webb PI, Ellison J (1998) Normothermy, torpor, and arousal in hedgehogs (erinaceus europaeus) from Dunedin. New Zeal J Zool 25:85–90. https://doi.org/10.1080/03014223.1998.9518139

Westman W, Geiser F (2004) The effect of metabolic fuel availability on thermoregulation and torpor in a marsupial hibernator. J Comp Physiol B Biochem Syst Environ Physiol 174:49–57. https://doi.org/10.1007/s00360-003-0388-y

Wilz M, Heldmaier G (2000) Comparison of hibernation, estivation and daily torpor in the edible dormouse, Glis glis. J Comp Physiol B Biochem Syst Environ Physiol 170:511–521. https://doi.org/10.1007/s003600000129

Withers PC (1977) Respiration, metabolism, and heat exchange of euthermic and torpid poorwills and hummingbirds. Physiol Zool 50:43–52